JOURNAL OF GUIDANCE, CONTROL, AND DYNAMICS
Vol. 18, No. 4, July–August 1995

Minimum-Time Reorientation of a Two-Degree-of-Freedom Gyroscope

Shmuel Boyarski* and Joseph Z. Ben-Asher†
Tel-Aviv University, Ramat Aviv 69978, Israel

The problem of time-optimal reorientation of the inner gimbal of a two-degree-of-freedom gimballed gyroscope mounted on a nonrotating base is considered. The states in the gyro model are the gimbals' angles (nutation is ignored). The model is nonlinear (not limited to small angles), state constrained, control limited, and double input, double output. A simple, explicit solution based on an intuitive observation is presented; it exploits the system's nonlinearity and channel coupling for attaining the minimum-time goal. It is analytically shown, in detail, that the solution satisfies the Maximum Principle and fulfills a sufficient condition for optimality based on the Hamilton–Jacobi–Bellman equation.

I. Introduction

THE 2-degree-of-freedom (DOF) gimballed gyroscope[1,2] is a complex mechanical/electronic instrument that is commonly used in control, navigation, sighting, and homing systems. It appears as a direction/attitude sensor, as a stabilized/controllable platform for other sensors, and, more recently, as a torque actuator for spacecraft.[3,4]

In this work, gyroscope control means control of the gimbals' angles (or control of the attitude of the inner gimbal and rotor relative to the gyroscope's base); it is physically accomplished by applying torques at the gimbals' axes. (Each gimbal is rotated by the torquer of the other axis, due to the precession phenomenon.) The control scheme is aimed at reorienting/slewing the inner gimbal or at attaining some desired gimbals' angles. Note that the spatial (absolute) orientation of the inner gimbal is geometrically (uniquely) related to the base orientation and the gimbals' angles. It is common practice to ignore the nutation in the control of large-angle movements. Slewing gyroscope-stabilized sighting/homing systems is a classical application.

Traditionally, gyroscope control is linear and "decoupled": Each gimbal angle is separately treated, without regard of the other angle, and a linear relation is assumed between the control torque and the respective angle rate of change. This approach is correct for small inner gimbal angles.

It seems that optimization and multi-input, multi-output (MIMO) treatment of gyroscope-related control have been motivated by the appearance of control moment gyroscopes (CMGs) in space applications. (CMGs are momentum-exchange actuators: torquing the gimbals changes the rotor orientation and produces a reaction torque on the host spacecraft.) Optimality refers, in Ref. 4, to the placement of the eigenvalues of the closed loop; in Ref. 5, to providing the shortest angular path between two orientations of the spacecraft eigenaxis; and in Ref. 3, to managing the CMG system redundancy so that undesirable rotor and gimbal orientations are avoided.

A somewhat related class of problems addresses minimum-time reorientation of spacecraft. Rigid-body, rest-to-rest, time-optimal rotational maneuvers are discussed in Refs. 6 and 7; singular solutions of this problem are emphasized in Ref. 8. In Ref. 9, the time-optimal slewing problem of flexible spacecraft is considered.

This paper directly attacks (for the first time, to the authors' best knowledge[10]) the problem of minimum-time reorientation of the rotor (and inner gimbal) of a "nutationless" 2-DOF gimballed gyroscope mounted on a nonrotating base. (Without this kinematic condition on the base the gyroscope's equations of motion are far more complicated.[2,10]) The problem is nonlinear and MIMO (2×2) because the cosine of the inner gimbal's angle appears in both state (gimbal angle) equations. Torque and angle constraints are taken into account.

Since the control torques applied to the gyroscope necessarily act on the gyroscope's base too, the nonrotating-base condition can hold only when the base's inertia is far greater than the gyroscope's inertia. A common situation answering these requirements involves a sighting sensor installed within the inner gimbal of a "small" 2-DOF gyroscope mounted on an aircraft flying straight and level. In such applications the minimum-time index (regarding sensor slewing) is of obvious operational importance. As for CMGs, they are intended to rotate their base (the spacecraft); thus, the base kinematic condition is not met by definition. However, our equations of motion may still be approximately valid if there is a sufficient time-scale difference between the "slow" rotations of spacecraft and the "fast" rotations of the CMG's gimbals. (In fact, minimum-time gimbals rotations contribute to the above time scale separation.) Shortening the time required for a desired rotor attitude change (with given, limited torquers) can be viewed as an increase in the maximum "effective torque" sensed by the spacecraft.

The treatment is purely analytic. Necessary and sufficient conditions for optimality are shown, for an intuitively derived solution, using the Pontryagin MP and the HJB equation. The solution is explicit, simple, and easy to implement. It should be emphasized that the nonlinearity and coupling are deliberately exploited for attaining the minimum-time goal.

II. Physical Configuration, System Definition, and Problem Formulation

An "ideal" conventional 2-DOF gyroscope is rigidly attached to a nonrotating base. (The base may have translational velocity and even translational acceleration.) The outer gimbal tilts through an angle θ; the inner gimbal tilts through an angle ψ. Here, $\dot{\theta} > 0$ means that the outer gimbal is "pitching up" relative to the base and $\dot{\psi} > 0$ means that the inner gimbal is "yawing to the right."

The gyroscope system includes two torquers and a constant-speed motor. The "outer" torquer produces the torque M_θ about the outer gimbal's (pitch) axis; the "inner" torquer produces M_ψ about the inner gimbal's (yaw) axis. The torquers are commanded by some control logic (in order to "level" the gyro with respect to the apparent gravity, to slew the inner gimbal in some desired direction, etc.). The constant-speed motor lies within the inner gimbal and maintains the rotor spin speed constant.

An ideal 2-DOF gyroscope is characterized[2] by lack of friction and the assumptions that all the pertinent elements' reference frames are inertia principal axes and that the center of gravity of the

Received Feb. 2, 1994; revision received March 25, 1994; accepted for publication Oct. 3, 1994.

*Graduate Student, Faculty of Engineering, Department of Electronic Systems.

†Adjunct Professor, Faculty of Engineering, Department of Electronic Systems.

gyroscope system lies at the gyroscope's nodal point and is independent of θ and ψ (no mass imbalance).

Neglecting nutation, the gimbal angle vector equation of motion is $\dot{x} = f(x, u)$, where the state vector is $x \doteq [\theta\ \psi]^T$ and the control vector is $u \doteq [u_\theta\ u_\psi]^T$. The two explicit scalar equations of motion are[1,2]

$$\dot{\theta} = u_\theta / \cos\psi \tag{1}$$

$$\dot{\psi} = u_\psi / \cos\psi \tag{2}$$

The above equations constitute an exact model of the first-order dynamics of the depicted gyroscope. Note that this is a state-nonlinear MIMO (2 × 2) system; θ is affected by ψ. The control of each axis is, essentially, the torque applied at the other axis (precession): $u_\theta = -M_\psi / h$, $u_\psi = M_\theta / h$. (h is the spin momentum of the gyro, i.e., the rotor spin speed times the rotor inertia about the spin axis.)

In practice, in order to preclude "gimbal-lock," the inner gimbal is always physically limited (by hard stops) to some ψ_L that is smaller than 90 deg so that, for any t, $|\psi(t)| \le \psi_L < \pi/2$. ($\psi_L$ designates the absolute value of the limiting ψ; the limit is assumed to be symmetric about $\psi = 0$.) The controls are also limited, of course. We denote the maximum absolute values of the controls by u_{θ_M} and u_{ψ_M} and the set of admissible controls by Ω_u; thus, $u \in \Omega_u$ means that (u_θ, u_ψ) belongs to $\{(u_\theta, u_\psi) \mid |u_\theta| \le u_{\theta_M}$ and $|u_\psi| \le u_{\psi_M}\}$.

At the initial time t_0 the system is in its initial condition $x_0 = [\theta_0\ \psi_0]^T$. The final state of the system, at the final time t_f, must be $x_f = [\theta_f\ \psi_f]^T$. It should be emphasized that neither end state is taken to be zero and that the only case explicitly excluded from our discussion is $\theta_f = \theta_0$, in which Eq. (1) is not effective and the problem is a trivial single-input, single-output (SISO) problem. The task is to find the control history $u(t) = [u_\theta(t)\quad u_\psi(t)]^T$ that transfers the system from x_0 to x_f in minimum time, i.e., to minimize t_f, subject to all the system constraints.

III. Proposed Solution

A. Concept and Formulas

Usually, the MP is used to find solutions for optimization problems. In this paper, however, the procedure is different. At first, we present four alternative "guessed" candidate trajectories that constitute the proposed optimal solution (in the to-be-defined θ-critical scenario): upper corner (UC), lower corner (LC), upper plateau (UP), lower plateau (LP). (See Figs. 1–3. Note that the state is defined as $x \doteq [\theta\ \psi]^T$ but Figs. 3 and 4 show a ψ-θ plane, i.e., ψ is drawn as the abscissa and points are denoted as (ψ, θ), because ψ usually indicates yawing.) Then, the MP and dynamic programming (DP) are employed to test whether the candidates are indeed optimal.

The notation used is standard. The state vector x and the control vector u have already been defined; we shall mostly refer to the elements of x, θ and ψ, and to the elements of u, u_θ and u_ψ. The costate vector is $\lambda \doteq [\lambda_\theta\ \lambda_\psi]^T$. When a trajectory acronym appears as a lower index, it indicates the type of trajectory or the "waypoint" to which a variable belongs; for example, t_{UC} is the time at which the corner occurs in the UC trajectory, ψ_{UC} is the value of ψ then, and $t_{f,UC}$ in the final time of the UC trajectory. When θ or ψ appear as lower indexes, they identify either the "channel" to which a vector element is related, as in u and λ, or the respective partial derivative of a variable. For example, λ_θ is the θ costate whereas J^*_θ is the θ derivative of the (scalar) optimal return function J^*. (J^*_x is composed, in our case, of J^*_θ and J^*_ψ; J^*_t is the time derivative of J^*.) Here, H stands for the Hamiltonian, a dot indicates a time derivative, and a star superscript is attached to any function associated with the (candidate) optimal solution. The class C^1 is of continuously differentiable functions; C^2 is the class of functions having continuous second (partial) derivatives. A bold centerdot indicates inner multiplication of vectors.

Our specific choice of candidates is motivated by the observation that "control effectiveness" is largest when $|\psi|$ is largest (since both state rates are proportional to 1/cos ψ); hence, time optimality must be associated with driving ψ away from zero as fast, as much, and as long as possible (while returning to ψ_f "on time," exactly when θ reaches θ_f). Physical interpretation: The gyroscope offers less resistance to an exerted control torque when the spin axis is farther from perpendicularity with the torque axis. Note that such ψ-manipulations can be performed only if some relative "slack" is available in the ψ channel, i.e., when "the θ channel is critical." (See Sec. III.B, comment 5.)

The four candidate trajectories, all comprised of constant-control "legs" only (with maximum u_θ and maximum or zero u_ψ), are tailored according to the above ψ-manipulation idea using the expressions given in Appendix 1, which are derived[10] directly from the equations of motion. The key features of the trajectories (control histories, timings, state waypoints, and applicability conditions) are summarized in Tables 1–4. An algorithm for applying the solution in a practical implementation is suggested afterwards.

B. Comments

1) For corner solutions to be valid, $|\psi_{UC}|$ and $|\psi_{LC}|$ must, of course, be smaller than ψ_L. ($\psi_{UC} > \psi_L$ implies an upper plateau; $\psi_{LC} < -\psi_L$ implies a lower plateau.)

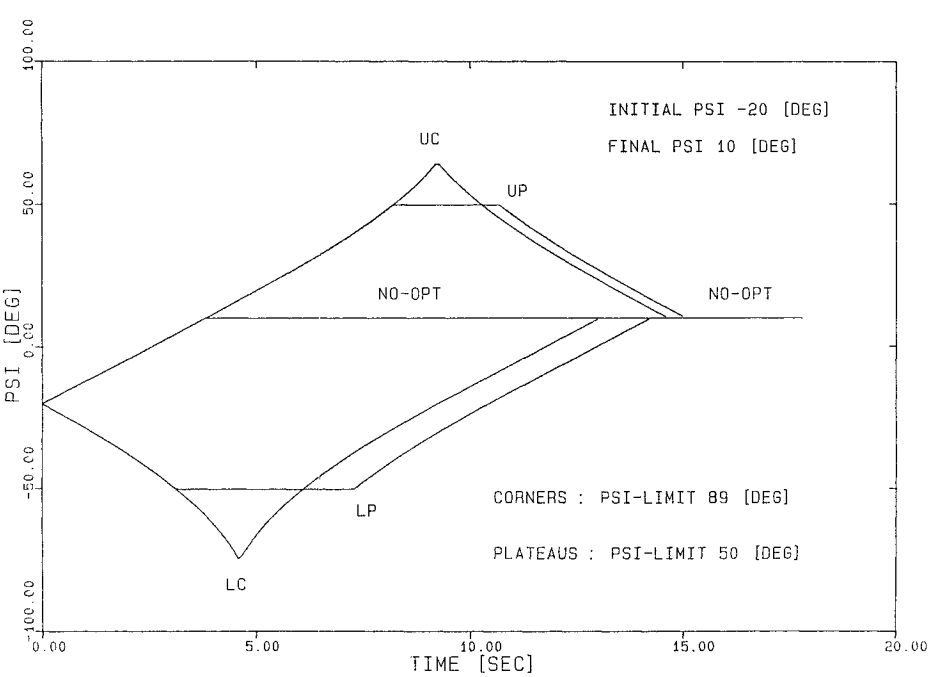

Fig. 1 ψ **time histories.**

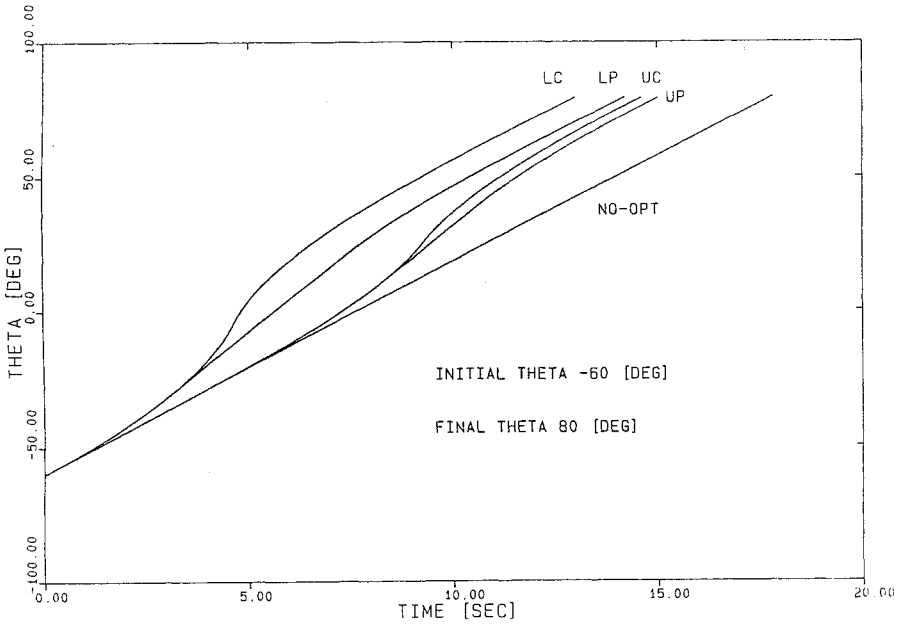

Fig. 2 θ **time histories.**

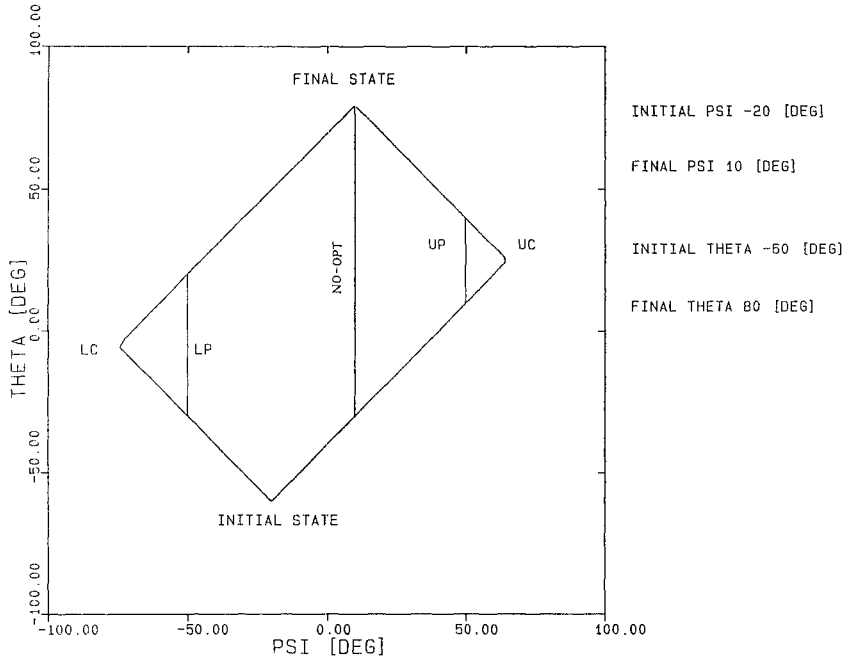

Fig. 3 ψ-θ **time histories.**

2) Figures 1–3 show the candidate trajectories for two different problems: The corners apply in the $\psi_L = 89$ deg case and the plateaus apply in the $\psi_L = 50$ deg case. [If ψ_L is between $|\psi_{UC}|$ and $|\psi_{LC}|$, the candidates are the plateau and possibly (see comment 10 below and remark 1 in Sec. IV.D) the corner.]

3) Figures 1–3 show also the trajectory ("no-opt") that results from applying simple "linear" control: in each axis there is a single "bang" that stops independently when its target angle is reached. Note the considerable time saving (relative to the conventional no-opt control) that the optimization achieves in these examples.

4) Interestingly, in these examples the better candidates (LC, LP) are those where ψ initially goes farther from ψ_f (i.e., the initial ψ control is opposite to the expected, "natural" direction).

5) It is impossible to reach ψ_f from ψ_0 with a single $\dot{\psi}$ sign change that occurs within the ψ band confined between ψ_0 and ψ_f. Therefore, ψ_{UC} represents a self-consistent UC trajectory only if $\max(\psi_0, \psi_f) < \psi_{UC}$; similarly, it is required that $\min(\psi_0, \psi_f) > \psi_{LC}$. Both these inequalities lead[10] to the following definition of θ as a "critical channel": $|\psi_f - \psi_0|/u_{\psi_M} < |\theta_f - \theta_0|/u_{\theta_M}$. If this does not hold in a specific problem, then the θ channel is not critical and no ψ-manipulation solution (UC, LC, UP, or LP) is required for attaining time optimality in that case. The condition $\theta_f \neq \theta_0$ is, in fact, covered by the latter inequality.

6) A geometric interpretation of $|\psi_f - \psi_0|/u_{\psi_M} < |\theta_f - \theta_0|/u_{\theta_M}$ (see Fig. 4): in the ψ-θ plane draw two straight lines of slopes $+u_{\theta_M}/u_{\psi_M}$ and $-u_{\theta_M}/u_{\psi_M}$ passing through the point (ψ_f, θ_f). (The final legs of the four candidates in Fig. 3 lie on these lines.) The locus of all the points (ψ_0, θ_0) that comply with the above inequality is the area of the two vertical wedges confined between these lines.

7) The two horizontal wedges created by the above lines are the locus of all the points (ψ_0, θ_0) from which the time-optimal solution consists of a single, independent bang in each axis (see comment 3 above); θ_f is reached first, and the second leg lies on the horizontal line $\theta = \theta_f$.

8) Moreover, the above straight lines are the locus of all possible corners; this is ascertained by the fact that the substitutions $\psi_{UC} = \psi_0$ and $\psi_{LC} = \psi_0$ (which make $t_{UC} = t_0$ and $t_{LC} = t_0$) degenerate both ψ-corner expressions into the equation $|\psi_f - \psi_0|/u_{\psi_M} = |\theta_f -$

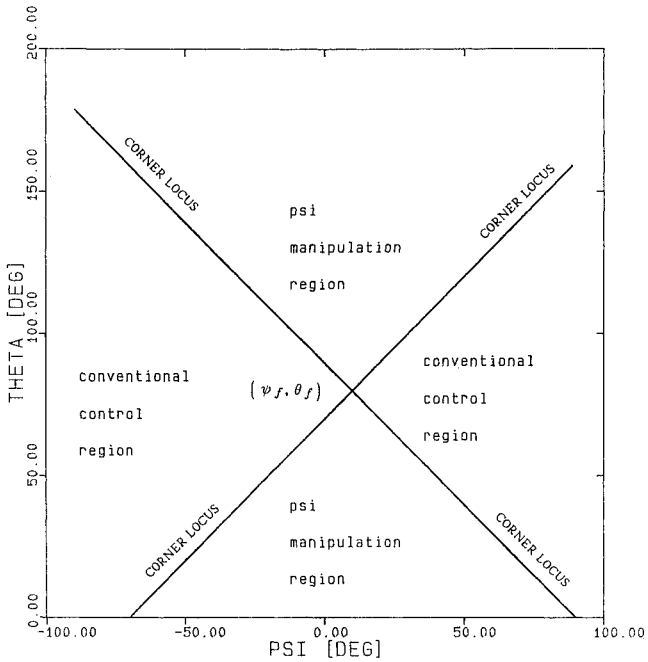

Fig. 4 Corner locus and conventional/manipulation regions.

$\theta_0|/u_{\theta_M}$. Therefore, if (ψ_0, θ_0) lies on these lines, the first corner leg is missing (i.e., the trajectory starts from the "corner") and the bangs in both axes, which constitute the candidate solution in this case, terminate simultaneously.

9) In the UP solution, the cases $t_{1,\mathrm{UP}} = t_0$ and $t_{2,\mathrm{UP}} = t_{f,\mathrm{UP}}$ represent "degenerate" UP trajectories that occur when either ψ_0 or ψ_f equals ψ_L; in these cases the first or third legs of the UP trajectory are "missing." (Similar statements apply to the LP solution.)

10) The conditions $\max(|\psi_0|, |\psi_f|) \le |\psi_{\mathrm{UC}}|$ and $\max(|\psi_0|, |\psi_f|) \le |\psi_{\mathrm{LC}}|$ arise from the minimization processes required by the MP and the HJB equation, as we later show. All the other entries in the tables are obtained without resort to optimal control theory.

11) The fact that the guessed candidates are of the "bang-bang" type should not be surprising since we face a minimum-time problem with state equations that are linear in the controls (hence the Hamiltonian is linear in the controls), and the controls are limited.

12) The identification of the locus of corners (comment 8) and the results given in Appendix 1 allow immediate geometric construction of candidate ψ-manipulation corner trajectories: progress from (ψ_0, θ_0) along a straight line of slope $+u_{\theta_M}/u_{\psi_M}$ until the locus of corners is met (at the straight line of the opposite slope); then proceed along the locus to (ψ_f, θ_f); repeat the construction starting with $-u_{\theta_M}/u_{\psi_M}$. (Note that these self-consistent corner trajectories create a parallelogram, with vertices at x_0, x_f, and the two corners.) Check the $|\psi|$ of both corner-locus meetings against $|\psi_0|$ and $|\psi_f|$ and disqualify any trajectory that does not comply with the MP (comment 10). In fact, the vertical wedges in the ψ-θ plane (comment 6) can easily be decomposed by inspecion into regions where both corners are extremals and regions where only one corner is an extremal.

13) If the first leg of the above constructions meets the vertical lines $\psi = \psi_L$ or $\psi = -\psi_L$ before the corner locus is met, proceed along that vertical line until the corner locus is met, then along the locus to (ψ_f, θ_f). See also comment 9 above. We shall later show that any such construction (plateau) is an extremal.

14) Another way of decomposing the ψ-θ plane is into regions throughout which a certain type of trajectory is preferable (has a smaller t_f); this must be done by computing t_f for each valid candidate (extremal) at each point in the plane. (For the given x_f, x_0 scans the plane.) Of course, such a selection by t_f is not required where only one extremal exists. (See the end of comment 12 and the following implementation section.) The borders between these regions are the lines across which the advantage shifts from one type of trajectory to another.

15) The fact that we can suggest, for each point in the ψ-θ plane, a control that will start an extremal trajectory (later we shall show actual optimality of the lesser-t_f trajectory) turns our proposed solution into a closed-loop optimal strategy.

Table 1 Upper corner

ψ At corner	$\psi_{\mathrm{UC}} = (\psi_0 + \psi_f + \lvert\theta_f - \theta_0\rvert u_{\psi_M}/u_{\theta_M})/2$
Applicability conditions	$\theta_f \neq \theta_0$
	$\lvert\psi_f - \psi_0\rvert/u_{\psi_M} < \lvert\theta_f - \theta_0\rvert/u_{\theta_M}$
	$\max(\lvert\psi_0\rvert, \lvert\psi_f\rvert) \le \lvert\psi_{\mathrm{UC}}\rvert$
Corner time	$t_{\mathrm{UC}} = t_0 + (\sin\psi_{\mathrm{UC}} - \sin\psi_0)/u_{\psi_M}$
Final time	$t_{f,\mathrm{UC}} = t_0 + (2\sin\psi_{\mathrm{UC}} - \sin\psi_0 - \sin\psi_f)/u_{\psi_M}$
ψ Control	$u_\psi(t) = u_{\psi_M}, t_0 \le t \le t_{\mathrm{UC}}$
	$u_\psi(t) = -u_{\psi_M}, t_{\mathrm{UC}} < t \le t_{f,\mathrm{UC}}$
θ Control	$u_\theta(t) = \mathrm{sign}(\theta_f - \theta_0)u_{\theta_M}, t_0 \le t \le t_{f,\mathrm{UC}}$

Table 2 Lower corner

ψ At corner	$\psi_{\mathrm{LC}} = (\psi_0 + \psi_f - \lvert\theta_f - \theta_0\rvert u_{\psi_M}/u_{\theta_M})/2$
Applicability conditions	$\theta_f \neq \theta_0$
	$\lvert\psi_f - \psi_0\rvert/u_{\psi_M} < \lvert\theta_f - \theta_0\rvert/u_{\theta_M}$
	$\max(\lvert\psi_0\rvert, \lvert\psi_f\rvert) \le \lvert\psi_{\mathrm{LC}}\rvert$
Corner time	$t_{\mathrm{LC}} = t_0 - (\sin\psi_{\mathrm{LC}} - \sin\psi_0)/u_{\psi_M}$
Final time	$t_{f,\mathrm{LC}} = t_0 - (2\sin\psi_{\mathrm{LC}} - \sin\psi_0 - \sin\psi_f)/u_{\psi_M}$
ψ Control	$u_\psi(t) = -u_{\psi_M}, t_0 \le t \le t_{\mathrm{LC}}$
	$u_\psi(t) = u_{\psi_M}, t_{\mathrm{LC}} < t \le t_{f,\mathrm{LC}}$
θ Control	$u_\theta(t) = \mathrm{sign}(\theta_f - \theta_0)u_{\theta_M}, t_0 \le t \le t_{f,\mathrm{LC}}$

Table 3 Upper plateau

ψ_L Encounter time	$t_{1,\mathrm{UP}} = t_0 + (\sin\psi_L - \sin\psi_0)/u_{\psi_M}$
ψ_L Departure time	$t_{2,\mathrm{UP}} = t_0 + (\sin\psi_L - \sin\psi_0)/u_{\psi_M}$
	$+ [\lvert\theta_f - \theta_0\rvert/u_{\theta_M} - (2\psi_L - \psi_f$
	$- \psi_0)/u_{\psi_M}]\cos\psi_L$
ψ At plateau	$\psi(t) = \psi_L, t_{1,\mathrm{UP}} \le t \le t_{2,\mathrm{UP}}$
Applicability conditions	$\theta_f \neq \theta_0$
	$\lvert\psi_f - \psi_0\rvert/u_{\psi_M} < \lvert\theta_f - \theta_0\rvert/u_{\theta_M}$
	$\psi_{\mathrm{UC}} > \psi_L$ (see Table 1 for ψ_{UC})
Final time	$t_{f,\mathrm{UP}} = t_0 + (2\sin\psi_L - \sin\psi_f - \sin\psi_0)/u_{\psi_M}$
	$+ [\lvert\theta_f - \theta_0\rvert/u_{\theta_M} - (2\psi_L - \psi_f$
	$- \psi_0)/u_{\psi_M}]\cos\psi_L$
ψ Control	$u_\psi(t) = u_{\psi_M}, t_0 \le t \le t_{1,\mathrm{UP}}$
	$u_\psi(t) = 0, t_{1,\mathrm{UP}} < t \le t_{2,\mathrm{UP}}$
	$u_\psi(t) = -u_{\psi_M}, t_{2,\mathrm{UP}} < t \le t_{f,\mathrm{UP}}$
θ Control	$u_\theta(t) = \mathrm{sign}(\theta_f - \theta_0)u_{\theta_M}, t_0 \le t \le t_{f,\mathrm{UP}}$

Table 4 Lower plateau

$-\psi_L$ Encounter time	$t_{1,\mathrm{LP}} = t_0 + (\sin\psi_L + \sin\psi_0)/u_{\psi_M}$
$-\psi_L$ Departure time	$t_{2,\mathrm{LP}} = t_0 + (\sin\psi_L + \sin\psi_0)/u_{\psi_M}$
	$+ [\lvert\theta_f - \theta_0\rvert/u_{\theta_M} - (2\psi_L + \psi_f + \psi_0)/u_{\psi_M}]\cos\psi_L$
ψ at plateau	$\psi(t) = -\psi_L, t_{1,\mathrm{LP}} \le t \le t_{2,\mathrm{LP}}$
Applicability conditions	$\theta_f \neq \theta_0$
	$\lvert\psi_f - \psi_0\rvert/u_{\psi_M} < \lvert\theta_f - \theta_0\rvert/u_{\theta_M}$
	$\psi_{\mathrm{LC}} < -\psi_L$ (see Table 2 for ψ_{LC})
Final time	$t_{f,\mathrm{LP}} = t_0 + (2\sin\psi_L + \sin\psi_f + \sin\psi_0)/u_{\psi_M}$
	$+ [\lvert\theta_f - \theta_0\rvert/u_{\theta_M} - (2\psi_L + \psi_f + \psi_0)/u_{\psi_M}]\cos\psi_L$
ψ Control	$u_\psi(t) = -u_{\psi_M}, t_0 \le t \le t_{1,\mathrm{LP}}$
	$u_\psi(t) = 0, t_{1,\mathrm{LP}} < t \le t_{2,\mathrm{LP}}$
	$u_\psi(t) = u_{\psi_M}, t_{2,\mathrm{LP}} < t \le t_{f,\mathrm{LP}}$
θ Control	$u_\theta(t) = \mathrm{sign}(\theta_f - \theta_0)u_{\theta_M}, t_0 \le t \le t_{f,\mathrm{LP}}$

C. Implementation

The following suggestion for organizing the details of the solution in a real-time software implementation emphasizes the theoretical aspects:

1) At first, check whether $|\psi_f - \psi_0|/u_{\psi_M} < |\theta_f - \theta_0|/u_{\theta_M}$ holds; if it does not hold, apply a bang towards the target angle in both channels.

2) If $|\psi_f - \psi_0|/u_{\psi_M} < |\theta_f - \theta_0|/u_{\theta_M}$ holds, compute ψ_{UC} and ψ_{LC}.

3) If $\psi_{UC} > \psi_L$, compute $t_{f,UP}$; else, check whether $\max(|\psi_0|, |\psi_f|) \le |\psi_{UC}|$ holds, and (only) if it does, compute $t_{f,UC}$.

4) Repeat the last steps in the "lower" sense; i.e., if $\psi_{LC} < -\psi_L$, compute $t_{f,LP}$; else, check whether $\max(|\psi_0|, |\psi_f|) \le |\psi_{LC}|$ holds, and if it does, compute $t_{f,LC}$.

5) Now compare the computed final times (all of which represent trajectories that satisfy the MP and the HJB equation); the smallest indicates the control strategy that should be applied. Notice that in each specific problem at most two candidates remain for this comparison since in the "up" sense there is either an UP or an UC and in the lower sense there is either a LP or a LC; and a corner-type trajectory may sometimes not satisfy the MP and the HJB equation.

The specific solution chosen by the above algorithm can be applied either by times only (open loop) or by some combination of times and measured angles. In a pure open-loop implementation, compute the other relevant key timings of the chosen solution (corner time, if it is an UC or a LC, t_1 and t_2 if it is an UP or a LP) and apply the pertinent u_θ and u_ψ according to these timings. Closed-loop features may be added to such an open-loop implementation by computing also the key angles of the chosen solution and making some decisions during the ensuing process (such as u_ψ switching, bang termination in each channel separately, or prevention of "bumping" into the physical ψ limit) by comparing them with the continuously measured angles.

Our overall solution to the optimization problem can also be applied in a full-scale closed-loop manner (see Sec. III.B, comments 14 and 15): when the target x_f is declared, perform the above selection algorithm (with $x_0 = x$) at each allowed point x in the ψ-θ plane; store the initial control of the selected solution for each x as $u^\bullet(x)$, or identify a suitable plane decomposition as described in Sec. III.B, comment 14; then, during the ensuing process, evoke $u^\bullet(x)$ according to the measured x (or according to the plane portion to which the measured x belongs). See also Sec. V.D.

The presentation of the solution is now complete. At this point we turn to the presentation of the proof, i.e., to showing that the solution satisfies necessary and sufficient conditions for optimality.

IV. Proof of Compliance with Maximum Principle

A. Organization and Preliminaries

Testing a guessed candidate-optimal solution for compliance with the MP requires knowledge of the costates of the proposed solution, in addition to the controls and the states. Table 5 presents the costates $\lambda_\theta(t)$ and $\lambda_\psi(t)$ for the proposed trajectories. The costates are tailored[10] using the expressions developed in Appendix 2. Later, these costates are incorporated into the Hamiltonian and the actual minimization required by the MP is carried out.

The form of the MP we employ is

$$[u_\theta^\bullet\ u_\psi^\bullet]^T = \underset{\substack{u_\theta, u_\psi \\ u \in \Omega_u}}{\operatorname{argmin}} \left[\lambda_\theta^\bullet \frac{u_\theta}{\cos\psi^\bullet} + \lambda_\psi^\bullet \frac{u_\psi}{\cos\psi^\bullet} \right] \tag{3}$$

Equation (3) stems from the general form of the MP, $u^\bullet = \operatorname{argmin}_u H(x^\bullet, \lambda^\bullet, u, t)$, where $u \in \Omega_u$ and $H = \lambda^T \bullet f + \lambda_0 g$ (where the constant λ_0, not to be confused with the initial costate vector, may be taken as unity); the associated cost is $J = h[x(t_f), t_f] + \int_{t_0}^{t_f} g[x(t), u(t), t]\,dt$, and we chose $g = 0$ and $h = t_f$ so that $J \doteq t_f$. The components of f are given by Eqs. (1) and (2).

The MP addresses a Hamiltonian based on the proposed "optimal" state and costate, not on any other x or λ; only u is varied in the indicated minimization. Thus, we shall construct all the following Hamiltonians with the costate histories of Table 5. (Explicit state histories are not needed, as we shall see.) The $\psi(t)$ that will appear in these Hamiltonians is, in fact, $\psi^\bullet(t)$.

In order that Ω_u is entirely screened (or "covered") in the minimum search required by the MP, we parameterize u_ψ and u_θ by K_ψ and K_θ as follows:

$$u_\psi = K_\psi u_{\psi_M}, \qquad -1 \le K_\psi \le 1 \tag{4}$$

$$u_\theta = \operatorname{sign}(\theta_f - \theta_0) K_\theta u_{\theta_M}, \qquad -1 \le K_\theta \le 1 \tag{5}$$

The various optimal controls $u_\psi^\bullet$ and $u_\theta^\bullet$ we have proposed in Tables 1–4 can thus be redefined by K_ψ and K_θ, which are $+1$, -1, or 0. For example, in the LP (Table 4) we have $K_\psi = -1$, $t_0 \le t \le t_{1,LP}$; $K_\psi = 0$, $t_{1,LP} < t \le t_{2,LP}$; $K_\psi = 1$, $t_{2,LP} < t \le t_{f,LP}$; and $K_\theta = 1$, $t_0 \le t \le t_{f,LP}$.

B. Compliance of Upper and Lower Corners with Maximum Principle

Using the UC entries of Table 5 and Eqs. (4) and (5) for "some" u_ψ and u_θ, we have the following:

1) $t_0 \le t \le t_{UC}$:

$$\begin{aligned} H_{UC}(x^\bullet, \lambda^\bullet, u, t) &= \lambda_\theta^\bullet \frac{u_\theta}{\cos\psi^\bullet} + \lambda_\psi^\bullet \frac{u_\psi}{\cos\psi^\bullet} \\ &= \left[-\operatorname{sign}(\theta_f - \theta_0) \frac{\cos\psi_{UC}}{u_{\theta_M}} \right] \frac{\operatorname{sign}(\theta_f - \theta_0) K_\theta u_{\theta_M}}{\cos\psi(t)} \\ &\quad + \left[\frac{\cos\psi_{UC} - \cos\psi(t)}{u_{\psi_M}} \right] \frac{K_\psi u_{\psi_M}}{\cos\psi(t)} \Longrightarrow H_{UC}(x^\bullet, \lambda^\bullet, u, t) \\ &= K_\theta \left[-\frac{\cos\psi_{UC}}{\cos\psi(t)} \right] + K_\psi \left[\frac{\cos\psi_{UC}}{\cos\psi(t)} - 1 \right], \qquad t_0 \le t \le t_{UC} \end{aligned} \tag{6}$$

Equation (6) is composed of two terms that are independent contributions to H_{UC}; the θ contribution is determined by K_θ and the ψ contribution is determined by K_ψ.

Now, $\cos\psi_{UC}/\cos\psi(t) > 0$ because ψ (including ψ_{UC}, of course) is limited to $|\psi| < 90$ deg. Therefore, the θ contribution K_θ $[-\cos\psi_{UC}/\cos\psi(t)]$ is obviously minimized by the (positive) largest possible K_θ, i.e., $K_\theta = 1$. Note that this agrees with the proposed $u_\theta^\bullet$ of Table 1.

Table 5 Costates histories

	t	$\lambda_\psi(t)$	$\lambda_\theta(t)$
UC	$t_0 \le t \le t_{UC}$	$[\cos\psi_{UC} - \cos\psi(t)]/u_{\psi_M}$	$-\operatorname{sign}(\theta_f - \theta_0)\cos\psi_{UC}/u_{\theta_M}$
	$t_{UC} < t \le t_{f,UC}$	$-[\cos\psi_{UC} - \cos\psi(t)]/u_{\psi_M}$	$-\operatorname{sign}(\theta_f - \theta_0)\cos\psi_{UC}/u_{\theta_M}$
LC	$t_0 \le t \le t_{LC}$	$-[\cos\psi_{LC} - \cos\psi(t)]/u_{\psi_M}$	$-\operatorname{sign}(\theta_f - \theta_0)\cos\psi_{LC}/u_{\theta_M}$
	$t_{LC} < t \le t_{f,LC}$	$[\cos\psi_{LC} - \cos\psi(t)]/u_{\psi_M}$	$-\operatorname{sign}(\theta_f - \theta_0)\cos\psi_{LC}/u_{\theta_M}$
UP	$t_0 \le t \le t_{1,UP}$	$[\cos\psi_L - \cos\psi(t)]/u_{\psi_M}$	$-\operatorname{sign}(\theta_f - \theta_0)\cos\psi_L/u_{\theta_M}$
	$t_{1,UP} < t \le t_{2,UP}$	$(t - t_{2,UP})\tan\psi_L$	$-\operatorname{sign}(\theta_f - \theta_0)\cos\psi_L/u_{\theta_M}$
	$t_{2,UP} < t \le t_{f,UP}$	$-[\cos\psi_L - \cos\psi(t)]/u_{\psi_M}$	$-\operatorname{sign}(\theta_f - \theta_0)\cos\psi_L/u_{\theta_M}$
LP	$t_0 \le t \le t_{1,LP}$	$-[\cos\psi_L - \cos\psi(t)]/u_{\psi_M}$	$-\operatorname{sign}(\theta_f - \theta_0)\cos\psi_L/u_{\theta_M}$
	$t_{1,LP} < t \le t_{2,LP}$	$-(t - t_{2,LP})\tan\psi_L$	$-\operatorname{sign}(\theta_f - \theta_0)\cos\psi_L/u_{\theta_M}$
	$t_{2,LP} < t \le t_{f,LP}$	$[\cos\psi_L - \cos\psi(t)]/u_{\psi_M}$	$-\operatorname{sign}(\theta_f - \theta_0)\cos\psi_L/u_{\theta_M}$

The ψ contribution is more interesting. In order that our proposed u^*_ψ for this arc ($+u_{\psi_M}$ or $K_\psi = 1$) will indeed minimize the term $K_\psi[(\cos\psi_{UC}/\cos\psi(t)) - 1]$, it is necessary that

$$|\psi(t)| \le |\psi_{UC}| \tag{7}$$

i.e., if at any moment during the first arc of an UC solution the absolute value of ψ exceeds the absolute value of ψ_{UC} (the arc's final ψ), then this arc does not comply with the MP and therefore the whole UC trajectory is not optimal. On the other hand, if Eq. (7) holds, then the ψ contribution is minimized by $K_\psi = 1$, the positive largest possible K_ψ (in agreement with the proposed u^*_ψ of Table 1) and the first arc of the proposed UC complies with the MP. In that case, the value of the (minimal) Hamiltonian is -1 [See Eq. (6) with $K_\theta = K_\psi = 1$] and is constant all along the arc. We shall soon see that Eq. (7) itself and similar results for K_θ and K_ψ are obtained for the second arc of the UC too, and also for the two arcs of the LC (with $|\psi_{LC}|$).

Remember also that $\psi(t)$ is monotonous within each arc so that Eq. (7) can be assured by checking $|\psi_{UC}|$ against the absolute values of the arc's endpoints only; for the first arc, checking whether $|\psi_0| \le |\psi_{UC}|$ suffices since the other endpoint is ψ_{UC} itself.

2) $t_{UC} \le t \le t_{f,UC}$:

Here, $H_{UC}(x^*, \lambda^*, u, t)$ of the UC's second arc is similarly found to be

$$H_{UC}(x^*, \lambda^*, u, t) = K_\theta\left[-\frac{\cos\psi_{UC}}{\cos\psi(t)}\right] - K_\psi\left[\frac{\cos\psi_{UC}}{\cos\psi(t)} - 1\right] \tag{8}$$

$$t_{UC} < t \le t_{f,UC}$$

Comparison to Eq. (6) shows that the former discussion (regarding the first arc) is applicable here too, except that the minimizing K_ψ is now the smallest possible K_ψ, $K_\psi = -1$.

Note that for the second arc, checking whether $|\psi_f| \le |\psi_{UC}|$ suffices to assure Eq. (7) since $\psi(t)$ is monotonous and the arc starts with ψ_{UC} itself. This observation can be combined with $|\psi_0| \le |\psi_{UC}|$, its counterpart from the first UC arc, to

$$\max(|\psi_0|, |\psi_f|) \le |\psi_{UC}| \tag{9}$$

which assures compliance with the MP for the whole UC trajectory. Note that Eq. (9), an outcome of the MP, is stronger than the UC self-consistency requirement $\max(\psi_0, \psi_f) < \psi_{UC}$ (see Sec. III.B, comment 5): If $\max(\psi_0, \psi_f) < \psi_{UC}$ holds, then an UC solution exists, but if Eq. (9) does not hold, this solution is not optimal. This can happen, for example, in an UC's first arc when $\psi_0 < 0$ and $\psi_0 < \psi_{UC}$ and $\psi_f < \psi_{UC} < -\psi_0$.

Condition (9) can perhaps be understood by recalling the previously mentioned dependence of the "control effectiveness" upon $|\psi|$ and realizing that a self-consistent UC trajectory [which satisfies $\max(\psi_0, \psi_f) < \psi_{UC}$] may still be ineffective if the corner is not associated with large $|\psi|$ (or, more precisely, larger than the $|\psi|$ provided by a monotonous progression from ψ_0 to ψ_f.)

The corresponding LC analysis is similar and leads to a similar result:

$$\max(|\psi_0|, |\psi_f|) \le |\psi_{LC}| \tag{10}$$

Equations (10) and (9) can be combined into

$$\max(|\psi_0|, |\psi_f|) \le \psi_C \tag{11}$$

where ψ_C stands for both ψ_{UC} and ψ_{LC}. Note the outstanding simplicity of Eq. (11), the end result of the application of the MP to the UC and LC solutions.

C. Compliance of Unconstrained Arcs of Upper and Lower Plateaus with Maximum Principle

The analysis of the unconstrained arcs of both the UP and the LP is essentially identical to the UC and LC analysis except that ψ_L replaces ψ_{UC}, $-\psi_L$ replaces ψ_{LC}, $t_{1,UP}$ (for the first arc) and $t_{2,UP}$ (for the third arc) replace t_{UC}, and $t_{1,LP}$ (first arc) and $t_{2,LP}$ (third arc) replace t_{LC}. An important difference, though, is that the counterpart of Eq. (11) for the unconstrained arcs of the plateau trajectories, i.e., $\max(|\psi_0|, |\psi_f|) \le |\psi_L|$, is fulfilled by definition because ψ_L is the greatest possible $|\psi|$; in other words, the unconstrained arcs of the plateaus automatically satisfy the MP. (The same occurs when ψ_{UC} happens to coincide with $+\psi_L$ and when ψ_{LC} coincides with $-\psi_L$.)

D. Compliance of Plateaus with Maximum Principle

The necessary condition for optimality of constrained arcs is that H is minimized (on the constraint) by u^* so that further reduction of H can only be attained by violating the constraint.

Applying this test on the constrained arc (plateau) of the UP solution, we have, from Table 5 and Eqs. (4) and (5) and $\psi(t) = \psi_L$,

$$H_{UP}(x^*, \lambda^*, u, t)$$

$$= \left[-\operatorname{sign}(\theta_f - \theta_0)\frac{\cos\psi_L}{u_{\theta_M}}\right]\frac{\operatorname{sign}(\theta_f - \theta_0)K_\theta u_{\theta_M}}{\cos\psi_L}$$

$$+ [(t - t_{2,UP})\tan\psi_L]\frac{K_\psi u_{\psi_M}}{\cos\psi_L} \Longrightarrow H_{UP}(x^*, \lambda^*, u, t)$$

$$= K_\theta[-1] + K_\psi\left[(t - t_{2,UP})\frac{\tan\psi_L u_{\psi_M}}{\cos\psi_L}\right], \qquad t_{1,UP} < t \le t_{2,UP} \tag{12}$$

The θ contribution is minimized by $K_\theta = 1$. As for the ψ contribution 1) $(t - t_{2,UP})$ is negative $\forall t \in (t_{t,UP}, t_{2,UP})$ so that the greatest K_ψ will minimize the ψ contribution and 2) $K_\psi > 0$ (i.e., $u_\psi > 0$) will cause violation of the constraint ($\psi > \psi_L$).

Thus, in order to minimize H_{UP} as much as feasible without constraint violation, K_ψ must be zero, in accordance with u^*_ψ of Table 3. Note also that choosing $K_\psi = 0$ makes H_{UP} constant $\forall t \in (t_{1,UP}, t_{2,UP}]$ and that the resulting value of the minimal H_{UP} is -1.

On the constrained arc (plateau) of the LP solution, $\psi(t) = -\psi_L$, we have

$$H_{LP}(x^*, \lambda^*, u, t) = K_\theta[-1] - K_\psi\left[(t - t_{2,LP})\frac{\tan\psi_L u_{\psi_M}}{\cos\psi_L}\right] \tag{13}$$

$$t_{1,LP} < t \le t_{2,LP}$$

In this case $K_\psi = 0$ is the smallest legitimate choice since a "better" H can only be attained by violating the constraint ($\psi < -\psi_L$) by applying $u_\psi < 0$.

The proof of compliance with the MP, for all our proposed trajectories, is now complete.

Remarks:

1) A corner-type solution may not fulfill the MP, whereas plateau-type solutions always fulfill the MP.

2) Without direct reference to t_f (or to $|\psi_C|$) it is not possible to discern among solutions that comply with the MP; there is no "measure" of compliance with the MP.

3) The switching functions in our problem (see Sec. III.B, comment 11) are $\lambda_\theta/\cos\psi$ and $\lambda_\psi/\cos\psi$, but since $\cos\psi > 0$, the costates themselves constitute the switching functions. (Compare the control entries in Tables 1–4 and the signs of the corresponding costate entries in Table 5.)

4) The derivation regarding the plateaus in Sec. IV.D is somewhat heuristic. A more rigorous proof, employing an augmented Hamiltonian, can be found in Ref. 10.

V. Dynamic Programming Perspective; Sufficiency

A. Preliminaries and Outline

Up to now, no claims of sufficiency have been made; the MP, the only theoretical tool used, constitutes only a (first-order) necessary condition for optimality. This section is devoted to the DP theory, which provides sufficient conditions for optimality via the HJB equation. The following paragraphs remind some basic DP definitions and results.

1. *Optimal Return Function*

Referring to the optimization problem of steering the dynamic system

$$\dot{x}(t) = f[x(t), u(t), t] \tag{14}$$

Table 6 Initial costates as obtained from ORFs

	$J^\bullet(\theta_0, \psi_0; t_0)$	$(\partial/\partial\psi_0)J^\bullet(\theta_0, \psi_0; t_0)$	$(\partial/\partial\theta_0)J^\bullet(\theta_0, \psi_0; t_0)$
UC	$t_{f,\mathrm{UC}}$	$[\cos\psi_{\mathrm{UC}} - \cos\psi_0]/u_{\psi_M}$	$-\mathrm{sign}(\theta_f - \theta_0)\cos\psi_{\mathrm{UC}}/u_{\theta_M}$
LC	$t_{f,\mathrm{LC}}$	$-[\cos\psi_{\mathrm{LC}} - \cos\psi_0]/u_{\psi_M}$	$-\mathrm{sign}(\theta_f - \theta_0)\cos\psi_{\mathrm{LC}}/u_{\theta_M}$
UP	$t_{f,\mathrm{UP}}$	$[\cos\psi_L - \cos\psi_0]/u_{\psi_M}$	$-\mathrm{sign}(\theta_f - \theta_0)\cos\psi_L/u_{\theta_M}$
LP	$t_{f,\mathrm{LP}}$	$-[\cos\psi_L - \cos\psi_0]/u_{\psi_M}$	$-\mathrm{sign}(\theta_f - \theta_0)\cos\psi_L/u_{\theta_M}$

from an arbitrary initial point (x_0, t_0) to a desired (fixed) target with minimal cost J,

$$J = J[x_0, u(t), t_0] = h[x(t_f), t_f] + \int_{t_0}^{t_f} g[x(t), u(t), t]\,\mathrm{d}t \qquad (15)$$
$$t_0 \le t \le t_f$$

an optimal return function (ORF) is associated with each point (x_0, t_0) from which such a (usually unique) optimal path starts; it is the (minimal) cost attained by the optimal path[11]:

$$J^\bullet[x_0, t_0] = \min_{u(t)} \left\{ h[x(t_f), t_f] + \int_{t_0}^{t_f} g[x(t), u(t), t]\,\mathrm{d}t \right\} \qquad (16)$$
$$t_0 \le t \le t_f$$

Note that every point along the path of an optimal solution is also the starting point of "another" optimal path (to the same target) that coincides with the respective part of the "original" solution (by Bellman's principle of optimality); hence, an ORF must actually be associated with any point (x, t) that lies on an optimal trajectory:

$$J^\bullet[x(t), t] = \min_{u(\tau)} \left\{ h[x(t_f), t_f] + \int_{t}^{t_f} g[x(\tau), u(\tau), \tau]\,\mathrm{d}\tau \right\} \qquad (17)$$
$$t \le \tau \le t_f$$

The subsequent expressions will refer to the last form of $J^\bullet$.

2. Hamilton–Jacobi–Bellman Equation

Here, $J^\bullet$ satisfies the HJB differential equation

$$J_t^\bullet[x(t), t] + \min_u H(x, J_x^\bullet, u, t) = 0 \qquad (18)$$

where $u \in \Omega_u$ and H is the DP Hamiltonian, defined as

$$H(x, J_x^\bullet, u, t) = g + J_x^{\bullet T} \bullet f$$
$$= g[x(t), u(t), t] + J_x^\bullet[x(t), t]^T \bullet f[x(t), u(t), t] \qquad (19)$$

[The only difference between Eq. (19) and the MP form $H(x, \lambda, u, t)$ is the appearance of $J_x^\bullet$ instead of λ.] The boundary condition is

$$J^\bullet[x(t_f), t_f] = h[x(t_f), t_f] \qquad (20)$$

3. Connection to Maximum Principle

When $J^\bullet \in C^2$ and there are no state constraints, the MP can be derived from the HJB equation.[11,12] The derivation reveals that

$$\lambda^\bullet(t) = J_x^\bullet[x^\bullet(t), t] \qquad (21)$$

on the optimal trajectory; that is, the costate of the optimal solution is the "state sensitivity" of the optimal cost.

4. Hamilton–Jacobi–Bellman Equation as Basis of Sufficient Condition for Optimality

The HJB equation is a necessary condition for optimality since it is developed with the assumption that $J^\bullet$ exists. Therefore, showing compliance of a proposed solution with the HJB equation may be an alternative to a MP compliance analysis. We choose, however, to employ the results of the preceding MP study to show that our solution satisfies the HJB equation within the framework of a sufficient condition.

Among the various HJB-equation-based sufficiency theorems available in the literature (e.g., Lee and Markus,[13] p. 348; Athans and Falb,[14] p. 357), we found Leitmann's decomposition Theorem (sufficiency Theorem 2 in Ref. 15) most adapted to our setting. The Leitmann paper addresses the system $\dot{x}(t) = f[x(t), u(t)]$, the autonomous version of Eq. (14), and the performance index $J = \int_{t_0}^{t_f} g[x(t), u(t)]\,\mathrm{d}t$, the autonomous version of Eq. (15) with $h \equiv 0$. The control u belongs to the set of bounded, piecewise-continuous functions of t whose values are in $\Omega_u \subset R^m$; g and all the components of f are in C^1 in R^n; X is some open set in R^n ; $x(t_f) \in T$, T being the given target set in X, where $T \cap \bar{X}$ may belong to the rim of X; $D = \{X_1, X_2, \ldots, X_K\}$ is a finite decomposition of X; and M is the set of the borders between the X_i.

The theorem states that the control $u^\bullet(t)$ with corresponding solution $x^\bullet(t)$, $t_0 \le t \le t_f^\bullet$, is optimal with respect to all the admissible controls $u(t)$ with corresponding solutions $x(t)$, $t_0 \le t \le t_f$, such that $x(t_f) \in T$ and $x(t) \in X\ \forall t \in [t_0, t_f)$, if there exists a decomposition D of X and a scalar function $J^\bullet$ that 1) is continuous on X; 2) agrees on each $\bar{X}_i$ with some function $J_i^\bullet$ that is of class C^1 on $\bar{X}_i$; and 3) is such that $\lim_{x \to x_f} J^\bullet(x) = 0$ for $x_f \in T$ and $x \in p \subset \bar{X}$, where p is a system trajectory generated by an admissible control, such that the following two conditions are satisfied: $H\{x^\bullet(t), J_x^\bullet[x^\bullet(t)], u^\bullet(t)\} = 0\ \forall t \in [t_0, t_f^\bullet)$, and $H\{x, J_x^\bullet(x), u\} \ge 0\ \forall u \in \Omega_u$ and $\forall x \in X$, where H is defined by Eq. (19). If $x^\bullet(t)$ or x belongs to M, these two conditions should hold for $J^\bullet = J_i^\bullet$ for all the X_i adjacent to the relevant border.

5. Outline of Dynamic Programming Analysis

After identifying the various proposed ORFs we show that Eq. (21) holds for our candidate solutions and that all our $J^\bullet$ are of class C^1; then, we show that our $J^\bullet$ satisfy the HJB equation (using results obtained in the MP study for a shortcut); at last, we check if all the above conditions of the sufficiency theorem are indeed satisfied by our candidate-optimal solutions.

B. Obtaining Costates from Optimal Return Functions

The cost of minimum-time problems is either t_f or $t_f - t_0$; our choice of g and h (see Sec. IV.A) makes $J = t_f$. [With $t_0 = 0$, t_f itself is the to-be-minimized trajectory duration. We refrained from taking t_0 to be zero merely because DP formulations specifically address the initial conditions (x_0, t_0).]

At this point the reader should realize that the t_f formulas presented in Tables 1–4 are actually our proposed ORFs [see Eq. (16)]; for example, $J_{\mathrm{UC}}^\bullet(\theta_0, \psi_0; t_0) = t_{f,\mathrm{UC}} = t_0 + [2\sin\psi_{\mathrm{UC}} - \sin\psi_0 - \sin\psi_f]/u_{\psi_M}$, where $\psi_{\mathrm{UC}} = [\psi_0 + \psi_f + |\theta_f - \theta_0|u_{\psi_M}/u_{\theta_M}]/2$ (see Table 1). Similarly, $J_{\mathrm{LC}}^\bullet(\theta_0, \psi_0; t_0) = t_{f,\mathrm{LC}}$ (Table 2), $J_{\mathrm{UP}}^\bullet(\theta_0, \psi_0; t_0) = t_{f,\mathrm{UP}}$ (Table 3), and $J_{\mathrm{LP}}^\bullet = (\theta_0, \psi_0; t_0) = t_{f,\mathrm{LP}}$ (Table 4).

The costates given in Table 5 were obtained by a lengthy derivation[10] based on the tools developed in Appendix 2. Equation (21) offers another procedure, namely to partially differentiate the proposed ORFs with respect to the state. We shall now pursue this method. For example, in the UC case we have [using $(\mathrm{d}/\mathrm{d}\alpha)|\alpha| = \mathrm{sign}(\alpha)$, $\alpha \ne 0$] $J_{\theta,\mathrm{UC}}^\bullet \doteq (\partial/\partial\theta_0)J_{\mathrm{UC}}^\bullet(\theta_0, \psi_0; t_0) = (\partial/\partial\theta_0)t_{f,\mathrm{UC}} = -\mathrm{sign}(\theta_f - \theta_0)\cos\psi_{\mathrm{UC}}/u_{\theta_M}$. Comparing with the respective λ_θ entry in Table 5, one sees that $\lambda_{\theta,\mathrm{UC}} = J_{\theta,UC}^\bullet$. (Remember that λ_θ is the θ costate whereas $J_\theta^\bullet$ is the θ derivative of the ORF $J^\bullet$.) Similarly, $J_{\psi,\mathrm{UC}}^\bullet \doteq (\partial/\partial\psi_0)J_{\mathrm{UC}}^\bullet(\theta_0, \psi_0; t_0) = (\partial/\partial\psi_0)t_{f,\mathrm{UC}} = (\cos\psi_{\mathrm{UC}} - \cos\psi_0)/u_{\psi M}$, which is identical to the respective λ_ψ entry in Table 5 with $t = t_0$; i.e., $\lambda_{\psi_0,\mathrm{UC}} = J_{\psi,\mathrm{UC}}^\bullet$.

The eight ORF state derivatives are summarized in Table 6; all of them are equal (at t_0) to the previously computed costates, as anticipated.

To conclude, we have shown in this section that our candidate-optimal solutions have the property $\lambda^\bullet(t_0) = J_x^\bullet[x^\bullet(t_0), t_0]$, which is a profound link between the HJB equation and the MP and which will play a central role in the sufficiency proof. Note also that:

1) The term λ_θ is constant in our problem.

2) The situation $\theta_f = \theta_0$ has been explicitly excluded from all our proposed ψ-manipulation solutions (because its optimal solution is merely a u_ψ bang); moreover, $\theta(t)$ proceeds monotonically from θ_0 to θ_f so that $\theta(t) \neq \theta_f$ for $t_0 \leq t < t_f$.

3) The eight first partial derivatives with respect to θ_0 and ψ_0 of the four candidate $J^\bullet$ are all continuous in θ_0 and ψ_0. The four first partial derivatives of the ORFs with respect to t_0 are unity (see the t_f in Tables 1–4.) Thus, all of our $J^\bullet$ are of class C^1 in all arguments.

4) In fact, all of our $J^\bullet$ are of class C^2; see Ref. 10. (Continuity of the second partial derivatives of the ORFs is a requirement of the Lee and Markus[13] sufficiency theorem, not of the Leitmann[15] theorem.)

5) Until now everything was taken at t_0; however, the above costate-$J^\bullet$ relations must hold at all subsequent (x, t) if our trajectories are indeed optimal, according to the principle of optimality. This can immediately be verified for the whole first leg of each trajectory: If ψ_0 is replaced by $\psi(t)$ in the $(\partial/\partial\psi_0)J^\bullet(\theta_0, \psi_0; t_0)$ entries, they become identical to first-leg $\lambda_\psi(t)$ entries of Table 5.

C. Compliance with Hamilton–Jacobi–Bellman Equation

This step, the cornerstone of the sufficiency proof, turns out to be easy thanks to the last results and the results of the MP analysis. We start by considering the Hamiltonian (19) that appears in the HJB equation (18).

In the MP analysis we defined $J = t_f$ by choosing $g = 0$ and $h = t_f$, so that the Hamiltonian used was $\lambda_\theta(u_\theta/\cos\psi) + \lambda_\psi(u_\psi/\cos\psi)$ [see Eq. (3)]. In the DP formulation we use the same g, so that our DP Hamiltonian is

$$0 + \begin{bmatrix} J_\theta^\bullet & J_\psi^\bullet \end{bmatrix} \begin{bmatrix} \dot\theta \\ \dot\psi \end{bmatrix} = J_\theta^\bullet\dot\theta + J_\psi^\bullet\dot\psi$$

or

$$H(x, J_x^\bullet, u, t) = J_\theta^\bullet \frac{u_\theta}{\cos\psi} + J_\psi^\bullet \frac{u_\psi}{\cos\psi} \tag{22}$$

As already noted, the DP Hamiltonian (22) is similar to the MP Hamiltonian; the only difference is the appearance of $J_\theta^\bullet$ and $J_\psi^\bullet$ instead of λ_θ and λ_ψ.

Now, recall that we have shown in Sec. V. B that all our candidate-optimal solutions have the property $\lambda^\bullet(t_0) = J_x^\bullet[x^\bullet(t_0), t_0]$; therefore, the above MP and DP Hamiltonians are indeed identical at the initial conditions. [Note that the costates λ_θ and λ_ψ were computed for any $t \in [t_0, t_f]$, whereas the optimal return functions $J^\bullet$ refer, by definition, to the initial conditions. Since $\lambda^\bullet = J_x^\bullet$ has been shown for (x_0, t_0) only, the Hamiltonian equality is strictly proven for the initial conditions only. However, the Hamiltonian equality must hold for any "downstream" point because of the principle of optimality.]

In the MP analysis we showed that the MP Hamiltonian is minimized by our proposed controls [i.e., Eq. (3) holds] at any time $t \in [t_0, t_f]$; moreover, the minimal MP Hamiltonian is at all times -1:

$$\min_{\substack{u_\theta, u_\psi \\ u \in \Omega_u}} \left(\lambda_\theta^\bullet \frac{u_\theta}{\cos\psi^\bullet} + \lambda_\psi^\bullet \frac{u_\psi}{\cos\psi^\bullet} \right) = -1 \tag{23}$$

The above arguments lead to the following conclusion, which holds for $t = t_0$, $\psi = \psi^\bullet = \psi_0$, and $\theta = \theta^\bullet = \theta_0$:

$$\min_{\substack{u_\theta, u_\psi \\ u \in \Omega_u}} \left(J_\theta^\bullet \frac{u_\theta}{\cos\psi^\bullet} + J_\psi^\bullet \frac{u_\psi}{\cos\psi^\bullet} \right) = -1 \tag{24}$$

Besides, the first partial derivative with respect to t_0 of all the $J^\bullet$ is unity (see Sec. V.B or Tables 1–4):

$$J_t^\bullet[x(t_0), t_0] = 1 \tag{25}$$

By virtue of the preceding two equations [and Eq. (22)] we can now claim that the HJB equation (18) is satisfied at the initial conditions by all our candidate solutions:

$$\underbrace{J_t^\bullet[\theta_0, \psi_0; t_0]}_{1, \text{ by Eq. (25)}} + \underbrace{\min_{\substack{u_\theta, u_\psi \\ u \in \Omega_u}} \left[J_\theta^\bullet \frac{u_\theta}{\cos\psi^\bullet} + J_\psi^\bullet \frac{u_\psi}{\cos\psi^\bullet} \right]}_{-1, \text{ at } [\theta_0, \psi_0; t_0], \text{ by Eq. (24)}} = 0 \tag{26}$$

Moreover, the initial conditions are arbitrary so that Eqs. (26) and (18) hold for any (x, t) from which a ψ-manipulation solution (which satisfies the MP) starts. (In fact, we can propose an extremal for any point in the ψ-θ plane; see Sec. III.B, comments 7 and 15.)

For completion, note that the boundary condition (20) is satisfied by definition, since we chose $J \equiv t_f$ and $h \equiv t_f$.

D. Fulfillment of Sufficient Condition for Optimality

First, note the following:

1) In the Leitmann sufficiency theorem (Sec. V.A.4) $h \equiv 0$ so that a minimum-duration cost must be defined by $g = 1$, as opposed to our $g = 0$ and $h = t_f$ choice for the MP analysis [see the paragraph after Eq. (3) and the beginning of Sec. V.B]. These two ways of posing a minimum-time index are equivalent, because minimizing $J_L = t_f - t_0$ (the cost associated with the Leitmann formulation) and minimizing $J = t_f$ are equivalent when t_0 is given.

2) The Leitmann sufficiency theorem addresses an autonomous system and a g that does not depend explicitly on t [$(J_L^\bullet)_t \equiv 0$]; under such circumstances the HJB equation (18) reduces to $\min_u H(x, J_x^\bullet, u) = 0$. (Compare to the two conditions on H of the theorem.)

3) Our system is indeed autonomous.

4) The costate histories of Table 5 can be obtained by a derivation similar to that in Ref. 10 but starting from $g = 1$ and $h = 0$; this can be ascertained by following the first steps of Appendix 2 with $H_L(x, \lambda, u) = \lambda^T \bullet f + \lambda_0 g = (\lambda_\theta u_\theta + \lambda_\psi u_\psi)/\cos\psi + 1$, where H_L is the Hamiltonian associated with the Leitmann theorem and $g = 1$. Note that $H_L = H + 1$.

For the above reasons, we may try the Leitmann sufficiency test on our solution.

Let us now review the detail requirements of the Leitmann sufficiency theorem and check whether they are all fulfilled by our solution:

1) The proposed control histories are bounded, piecewise-continuous functions of time and do not violate the control constraints; all our $u^\bullet(t)$ steer the system from the initial condition to the target and the trajectories do not violate the state constraints.

2) The state equations and the integrand of the cost function are continuous and possess continuous first derivatives with respect to all their arguments.

3) The open set X in R^2 (the ψ-θ plane) is $\{(\theta, \psi) \mid |\theta| < \pi, |\psi| < \psi_L\}$.

4) The decomposition D is the decomposition of X described in Sec. III.B, comment 14: Throughout each $\bar X_i$ one type of extremal has the smallest t_f (for a given x_f); the same extremal type may also characterize (by having the smallest $J^\bullet$) other, nonadjacent $\bar X_i$: the horizontal wedges confined between the two straight lines that are the locus of the corners (see Sec. III.B, comments 6 and 7) comprise one $\bar X_i$.

5) The existence of $J_i^\bullet \in C^1$ in each $\bar X_i$ is assured by the above method of decomposing X and the nature of our $J_i^\bullet$ ($i = UC, LC, UP, LP$), including the $J^\bullet$ of the conventional control that prevails in the horizontal wedges.

6) The "overall" $J^\bullet$, which coincides on each $\bar X_i$ with the applicable $J_i^\bullet$, is continuous on X since any borderline between two adjacent $\bar X_i$ corresponds to equality of the two $J_i^\bullet$ defining these $\bar X_i$; in fact, the borders are found by such equalities. Another way of describing $J^\bullet$ is $J^\bullet = \min(J_1^\bullet, J_2^\bullet)$ (remember that at most two extremals can compete in each x); the continuity of $J^\bullet$ is assured by the continuity of $J_1^\bullet$ and $J_2^\bullet$ and the nature of the min operator.

7) For any $x_f \in \bar X$ and $x \in \bar X$, $\lim_{x \to x_f} J^\bullet(x) = 0$ is true, as can be verified by substituting $\psi_0 = \psi_f$ and $\theta_0 = \theta_f$ in the four t_f expressions and realizing that $J_L^\bullet(x_f) = t_f|_{x_0 = x_f} - t_0 = t_0 - t_0 = 0$. [The external boundary (rim) of X arouses no irregularity in our case.]

We now turn to the conditions on H. We have shown in Sec. V. C. that all our proposed J^* satisfy the HJB equation and its associated boundary condition. Let us reinterpret Eqs. (24) and (26) in terms of the H_L and J_L associated with the Leitmann theorem and in regard to both the theorem conditions on H. As already noted, for the Leitmann autonomous formulation the HJB equation (18) takes the form $\min_u H_L(x, (J_L^*)_x, u) = 0$, or

$$\min_{u_\theta, u_\psi} \left[(J_L^*)_\theta \frac{u_\theta}{\cos\psi} + (J_L^*)_\psi \frac{u_\psi}{\cos\psi} + 1 \right] = 0 \tag{27}$$

Since the state derivatives of $J^*(\theta, \psi; t)$ and of $J_L^*(\theta, \psi)$ are identical, and since the 1 (which in this case originates from $\lambda_0 g$, not from J_t^*) does not participate in the minimization, the HJB equation becomes

$$\min_{u_\theta, u_\psi} \left(J_\theta^* \frac{u_\theta}{\cos\psi} + J_\psi^* \frac{u_\psi}{\cos\psi} \right) + 1 = 0 \tag{28}$$

Now, realize that in Sec. V.C it was shown [see Eqs. (24) and (26)] that we can fulfill Eq. (28) at any point in the ψ-θ plane by the u^* associated with some extremal (of the ψ-manipulation type, full or degenerate, or of the conventional type). This directly answers the second Leitmann condition on H: At any $x \in X$, $H_L(x, (J_L^*)_x, u)$ [the bracketed term on the left side of Eq. (27)] equals zero with the u^* corresponding to the applicable J_i^* (sometimes also with the u^* of the second valid extremal) and is positive with any other $u \in \Omega_u$. Thus, the first Leitmann condition on H, $H_L\{x^*(t), (J_L^*)_x[x^*(t)], u^*(t)\} = 0$, is also fulfilled, and not merely along the candidate trajectory [i.e., $\forall t \in [t_0, t_f^*)$, as shown in Sec. IV] but even pointwise. In short, since we have argued that (θ_0, ψ_0) of Eq. (26) may be any point in $\bar{X}$ (see Sec. III.B, comment 15), and since we showed that our proposed $u^*(t)$ are the minimizing controls [i.e., fulfill Eq. (3)], we can now claim that both Leitmann conditions on H_L are satisfied.

The proof that our proposed control strategy fulfills a sufficient condition for optimality is now complete. Interestingly, the theorem cannot discern the "best" among the valid extremals; it "only" assures us that by simply choosing our candidate solution that has the least t_f (and, of course, also satisfies the MP necessary condition for optimality) we obtain the true global minimum.

VI. Summary

The contribution of this work is an analytically proven, practical solution to the optimal control problem of transferring the state (gimbals' angles) of an inertially based, nutationless, 2-DOF gimballed gyroscope from a given initial condition to a desired target in minimum time. The gyroscope model is not limited to small inner gimbal angles. State constraints and control limitations are observed.

It seems that the above specific control problem has never been addressed before. The approach whereby the control scheme takes advantage of the inherent nonlinearity and channel coupling of the gyroscope, rather than fight them, is unconventional. (In fact, the solution drives the system away from its linear regime in order to enhance the "control effectiveness.") The purely analytical treatment and the attainment of a sufficiency proof for such a nonlinear MIMO problem are especially appealing.

The solution can readily be applied to large-angle slewing of gyroscope-platformed sighting systems, for example; its implementation in the control of spacecraft angular maneuvers requires adaptation to host rotations.

Appendix 1: Generic State Histories

The various trajectories are constructed using the following expressions, which emanate directly from the equations of motion (1) and (2); see Ref. 10:

1) With $t_0 = 0$ and constant u_ψ, the $\psi(t)$ trajectory leaving the initial condition is $\sin\psi(t) = \sin\psi_0 + u_\psi t$. The ψ trajectory arriving at the final condition with constant u_ψ is $\sin\psi(\tau) = \sin\psi_f - u_\psi \tau$, where $\tau \doteq t_f - t$.

2) The respective θ trajectories at these situations (with constant u_θ also) are $\theta(t) = \theta_0 + [\psi(t) - \psi_0]u_\theta/u_\psi$ and $\theta(\tau) = \theta_f + [\psi(\tau) - \psi_f]u_\theta/u_\psi$.

3) When $u_\psi = 0$ for $t \in [t_1, t_2]$, $t_0 \le t_1 \le t_2 \le t_f$, $\psi(t)$ is constant: $\psi(t) = \psi(t_1) \doteq \psi_1 = \psi_2$, $t_1 \le t \le t_2$.

4) The θ trajectory when $u_\psi = 0$ for $t \in [t_1, t_2]$ is $\theta(t) = \theta_1 + (t - t_1)u_\theta/\cos\psi_1$, where $\theta(t_1) = \theta(\tau_1) \doteq \theta_1$ and $u_\theta = $ const: and with regressing time: $\theta(\tau) = \theta_2 - (\tau - \tau_2)u_\theta/\cos\psi_2$, where $\theta(\tau_2) = \theta(t_2) \doteq \theta_2$.

These expressions suffice to develop the four candidate trajectories, which are all comprised of constant-control "legs."

Appendix 2: Generic Costate Histories

The following expressions and observations are used in the costate development:

1) The Hamiltonian of the problem is $H = \lambda_\theta u_\theta/\cos\psi + \lambda_\psi u_\psi/\cos\psi$; the costate equations are $\dot{\lambda}_\theta = -\partial H/\partial\theta$ and $\dot{\lambda}_\psi = -\partial H/\partial\psi$. Since θ does not appear explicitly in H, the $\dot{\lambda}_\theta$ equation implies that $\lambda_\theta(t) = \lambda_\theta = $ const (θ is "ignorable").

2) In order to trace λ_ψ, let us rewrite H as $H = (\lambda_\theta u_\theta + \lambda_\psi u_\psi)/\cos\psi$ and realize that $\partial H/\partial\psi = (\lambda_\theta u_\theta + \lambda_\psi u_\psi)(\sin\psi/\cos^2\psi) = H\tan\psi$; therefore, $\dot{\lambda}_\psi(t) = -H\tan\psi$.

3) The transversality condition at t_f is $H(t_f) = -1$. Since t does not appear explicitly in H ($\partial H/\partial t = 0$), we see that $H(t) = H(t_f)\ \forall t \in [t_0, t_f]$, or $H(t) = -1$. Substitution of this H into $\dot{\lambda}_\psi(t) = -H\tan\psi$ yields $\dot{\lambda}_\psi(t) = \tan\psi(t)$, or $\lambda_\psi(t) = \lambda_{\psi_0} + \int_{t_0}^{t} \tan\psi(\tau)\,d\tau$, where $\lambda_{\psi_0} = \lambda_\psi(t_0)$.

4) The last integral can be converted into a direct integral on ψ (for $u_\psi \neq 0$) as follows:

$$\int_{t_0}^{t} \tan\psi(\tau)\,d\tau = \int_{\psi_0}^{\psi} \left[\frac{\tan\xi}{d\xi/dt} \right] d\xi$$

$$= \int_{\psi_0}^{\psi} \left[\frac{\tan\xi}{u_\psi/\cos\xi} \right] d\xi = \int_{\psi_0}^{\psi} \frac{\sin\xi}{u_\psi}\,d\xi$$

Thus, λ_ψ can be rewritten as

$$\lambda_\psi(t) = \lambda_{\psi_0} + \int_{\psi_0}^{\psi} \frac{\sin\xi}{u_\psi} d\xi, \qquad u_\psi \neq 0$$

5) Further development of $\lambda_\psi(t)$ is possible in the case of constant u_ψ:

$$\int_{\psi_1}^{\psi_2} \frac{\sin\xi}{u_\psi}\,d\xi = \frac{\cos\psi_1 - \cos\psi_2}{u_\psi}$$

Here, $\psi_1 = \psi(t_1)$, $\psi_2 = \psi(t_2)$, and $u_\psi(t)$ is constant ($\neq 0$) during $t \in [t_1, t_2]$. Thus, $\lambda_\psi(t_2) = \lambda_\psi(t_1) + (\cos\psi_1 - \cos\psi_2)/u_\psi$, $t_2 \ge t_1$, $u_\psi = \text{const} \neq 0$.

6) If $u_\psi = 0$ during $t_1 \le t \le t_2$, it follows from the equations of motion that ψ is constant in that time interval: $\psi(t) = \psi_1 = \psi_2$. Then, $\int_{t_1}^{t_2} \tan\psi(\tau)\,d\tau = \tan\psi_1(t_2 - t_1)$ and $\lambda_\psi(t_2) = \lambda_\psi(t_1) + \tan\psi_1(t_2 - t_1)$, $t_2 \ge t_1$, $u_\psi = 0$.

It should be realized that, given a piecewise-constant $u_\psi(t)$, the above expressions enable a direct (though lengthy) computation of $\lambda_\theta(t)$ and $\lambda_\psi(t)$; see Ref. 10. [A further condition is required for the junctions of constrained and unconstrained arcs of the plateaus; see (3.13.4), (3.13.5), and (3.11.6) in Ref. 16.]

Acknowledgment

The authors are indebted to the reviewer who referred us to Ref. 15.

References

[1]Arnold, R. N., and Maunder, L., *Gyrodynamics and Its Engineering Application*, Academic, New York, 1961.

[2]Boyarski, S., "Exact and Approximate Equations of Motion of an Ideal Two-Degrees-of-Freedom Gimballed Gyroscope Attached to a Non-Inertial Base," *Proceedings of the Twenty-Third Israel Conference on Mechanical Engineering* (Haifa, Israel), 1990, Paper 6.3.1.

[3]Paradiso, J. A., "Global Steering of Single Gimballed Control Moment Gyroscopes Using a Directed Search," *Journal of Guidance, Control, and Dynamics*, Vol. 15, No. 5, 1992, pp. 1236–1244.

[4]Sunkel, J. W., and Shieh, L. S., "Optimal Momentum Management Controller for the Space Station," *Journal of Guidance, Control, and Dynamics*, Vol. 13, No. 4, 1990, pp. 659–668.

[5]Wie, B., Weiss, H., and Arapostathis, A., "Quaternion Feedback Regulator for Spacecraft Eigenaxis Rotations," *Journal of Guidance, Control, and Dynamics*, Vol. 12, No. 3, 1989, pp. 375–380.

[6]Bilimoria, K. D., and Wie, B., "Time-Optimal Three-Axis Reorientation of a Rigid Spacecraft," *Journal of Guidance, Control, and Dynamics*, Vol. 16, No. 3, 1993, pp. 446–452.

[7]Chowdhry, R. S., and Cliff, E. M., "Optimal Rigid Body Reorientation Problem," AIAA Paper 90-3485, Aug. 1990.

[8]Seywald, H., and Kumar, R. R., "Singular Control in Minimum Time Spacecraft Reorientation," *Journal of Guidance, Control, and Dynamics*, Vol. 16, No. 4, 1993, pp. 686–694.

[9]Ben-Asher, J., Burns, J. A., and Cliff, E. M., "Time-Optimal Slewing of Flexible Spacecraft," *Journal of Guidance, Control, and Dynamics*, Vol. 15, No. 2, 1992, pp. 360–367.

[10]Boyarski, S., "Time-Optimal Reorientation of a Two-Degrees-of-Freedom Gyroscope," M.S. Thesis, Tel-Aviv Univ., Israel, 1993.

[11]Kirk, D. E., *Optimal Control Theory: An Introduction*, Prentice–Hall, Englewood Cliffs, NJ, 1970.

[12]Pontryagin, L. S., Boltyanskii, V. G., Gamkrelidze, R. V., and Mishchenko, E. F., *The Mathematical Theory of Optimal Processes*, Wiley-Interscience, New York, 1962.

[13]Lee, E. B., and Markus, L., *Foundations of Optimal Control Theory*, Krieger, Malabar, FL, 1986.

[14]Athans, M., and Falb, P. L., *Optimal Control: An Introduction to the Theory and Its Applications*, McGraw–Hill, New York, 1965.

[15]Leitmann, G., "Sufficiency Theorems for Optimal Control," *Journal of Optimization Theory and Applications*, Vol. 2, No. 5, 1968, pp. 285–292.

[16]Bryson, A. E., Jr., and Ho, Y. C., *Applied Optimal Control: Optimization, Estimation and Control*, Wiley, New York, 1975.